



MINISTRY OF RESEARCH AND INNOVATION
NATIONAL INSTITUTE OF RESEARCH-DEVELOPMENT FOR
ELECTROCHEMISTRY AND CONDENSED MATTER
– INCEMC – TIMIȘOARA
300569, Timișoara, str. Dr. Aurel Păunescu Podeanu, no.144,
Tel./Fax: 0256 222119 / 0256 201382, e-mail: incemc@incemc.ro



Scientific-Technical Report

PED123/2017 Research Grant

„FULLERENE BASED DOUBLE-GRAPHENE PHOTOVOLTAICS”

Grant Director: Prof. dr. dr.-habil. CS1 Mihai V. PUTZ

Year 2017

Background and Mission

The experimental demonstration framework of the fullerene based double graphene photovoltaics (FG2PV) effect and product is fully supported by the exclusive top facilities in nano-sciences offered by the Laboratory of renewable energies – photovoltaics (LERF) hosted by INCEMC-Timisoara.

The project is supported by the promising hot results of experimentally obtaining and confirming of ozopolymeric fullerene based graphene, as well as the computationally prediction of enhancing of quantum signals (by bondons for graphene layers, and by bondots for inter-layers of graphene) due to the topo-defects propagation on graphene, which can be triggered by interaction with light as in photovoltaics.

It nevertheless should provide a scientific leap in the field of quantum dot photovoltaics, while offering an innovative route at regional, national and international levels for inclusively employing the green carbon nanostructures (as graphene is by default) with the nano-techniques and systems in renewable energies, the solar one in particular.

The main directions of research on 2017

1. Topological studies of monolayer graphene and of its precursors, mainly experimentally (by HRTEM morphology), yet with a reliable computational reference (chemical graphs of graphenic cells and super-cells);
2. Obtaining systematic metrology (Raman spectra, AFM) signals for monolayer graphenic flakes as obtained by fullerene temperature controlling cracking;
3. Predicting the photovoltaic properties from the measured signals at the points 1 and 2 above, through employing the quasi-quantum particles as bondons formed on the graphenic mono-layers;
4. Exploring the green application of graphenic monolayers though its bondonic properties eventually controlled within the preceding point 3.

Scientific Progress

Structural topology and HRTEM morphology of graphenic flakes

Graphene sheets are two-dimensional lattices, where the Carbon atoms represent the main vertices of the structure. These “sheets” represent the basic structure of fullerenes and other nano-carbon-structures (cylinders, ellipsoids, etc.) and also the basic structure of nanocones. Nanocones are in fact infinite Carbon lattices built by the infinite addition of hexagonal cells with Carbon vertices to a pentagonal carbonic cell. The structures can be considered as indefinitely large polycyclic aromatic hydrocarbons [1].

Page | 2

For a better understanding of the topological assessment of a graphene, we will make in the following some calculations on a graphene fragment. The fragment will be assessed as a “closed” fragment (**Figure no. 1**) and as an “open” one (**Figure no. 2**).

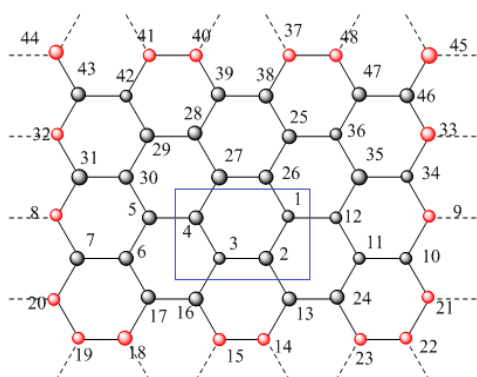


Figure 1. Closed graphene fragment. The four vertices placed in the blue rectangle are forming the unit that can be translated in the graph; the light colored marginal vertices are connected with the correspondent one on the opposite side of the unfolded lattice [2,3]

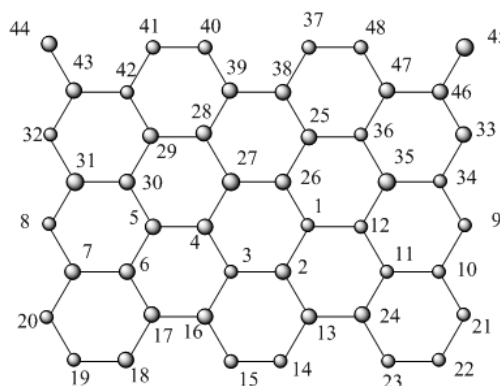


Figure 2. Open graphene fragment [2,3]

The idea of “topological compactness” mentioned by Ori, O., Putz, M.V. and coworkers [2,3] is demonstrated to be respected in the two examples above. So, chemical structures are more compact and probably they will prove to be more physical-chemical stable as their Wiener index decreases:

$$W(G, n) = \frac{1}{2} \sum_{ij} d_{ij}(1)$$

where $i, j = 1, \dots, n$ and d_{ij} is the shortest path between vertices i and j (the lowest number of edges connecting them) [4,5].

On the other side, the dual representation of the graphene can be used when studying topology of fullerenes or graphene “honeycomb” lattices with defects like insertions of pentagons/heptagons in the hexagonal net, isomerisations of the lattice by redistribution of edges between vertices. Together with coloring methods (coloring of the dual representations of the cells – like in **Figures 3 and 4** – blue for hexagons, red for pentagons and green for heptagons), the dual representation facilitates the topological studies or the studies of defect propagation in a

lattice. The redistribution of edges between vertices initially unconnected will rearrange the proximity (connectivity) of the cells and this can be very well seen in the dual lattice.

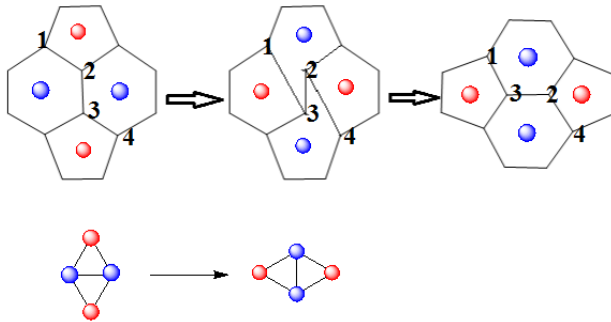


Figure 3. Isomerisation in a graph – “2-switch”/”diagonal flip”/”Stone-Wales” type. Direct and Dual graph representation (inspired by Babić, D., Ori, O. and their coworkers [6,7])

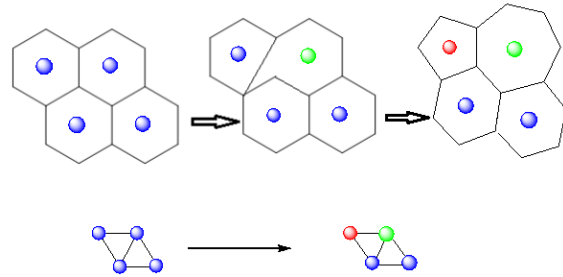


Figure 4. Isomerisation in a graph – Redistribution of an edge. Direct and Dual graph representation [6,7]

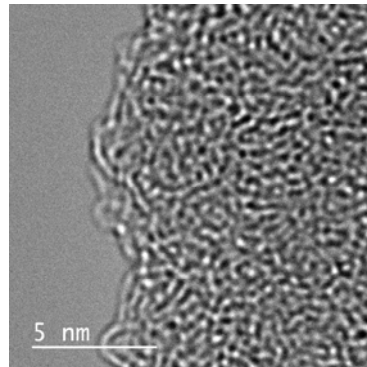
The coalescence processes of fullerenes and nanotubes also involve these isomerisations. Stone-Wales transformations also can propagate in a graphenic structure, these propagations being called Stone-Wales waves [8]. Such isomerisation mechanisms may broadly explain the observed HRTEM films as obtained from graphene oxide obtained by a novel method using fullerene ozopolymers [9-11], as presented in the Figures of the Table 1.

Table 1. The HRTEM photographs for the main probes under study in the actual PED123 research [12].

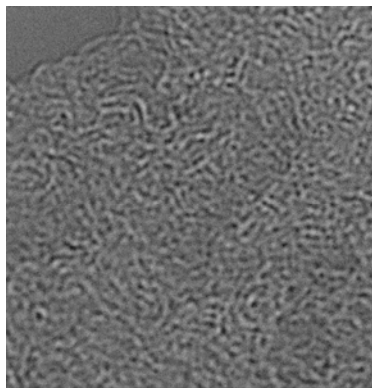
Probe

HRTEM of interest

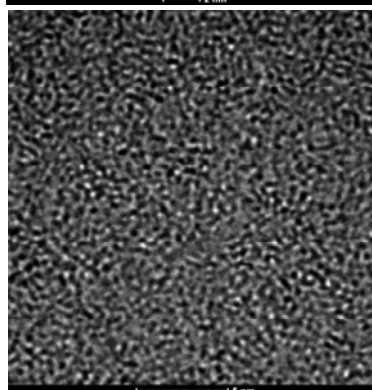
105-30_Pristine GO



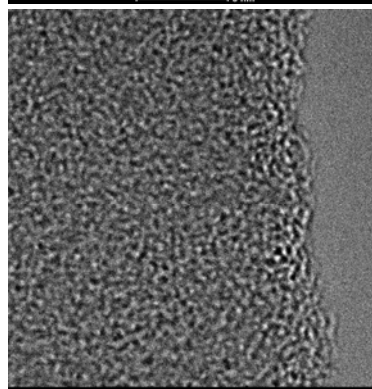
70-39_GO_630_N2



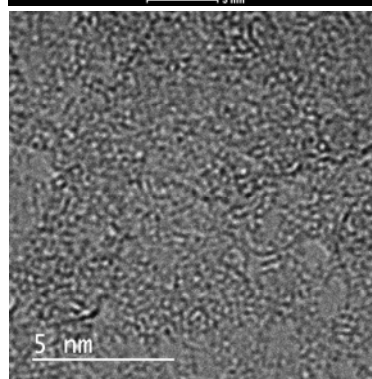
70-39_GO_DSC_350_N2



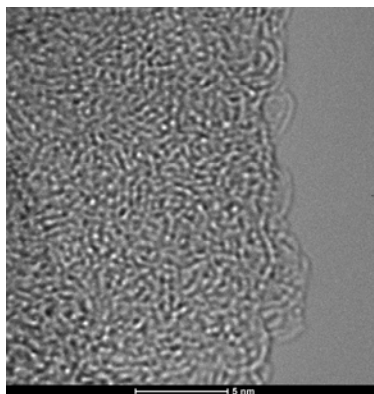
71-39_GO_105-30_DSC_450_N2



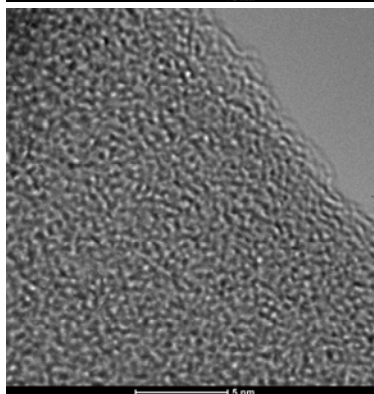
105-30_ref



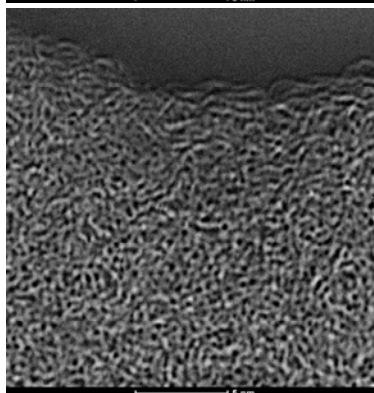
65-34_C70_Ozonide



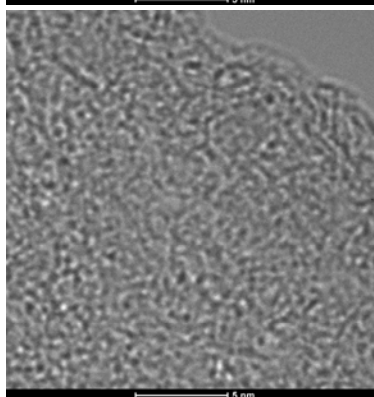
70-39_C60_Ozopolym_350_DSC



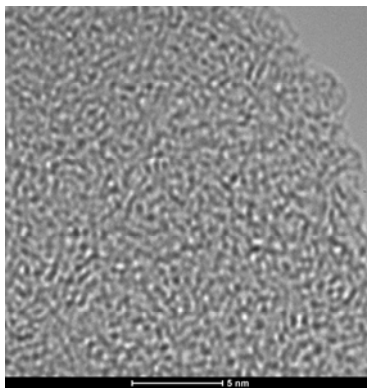
70-39_C70_Ozopolym_350_DSC



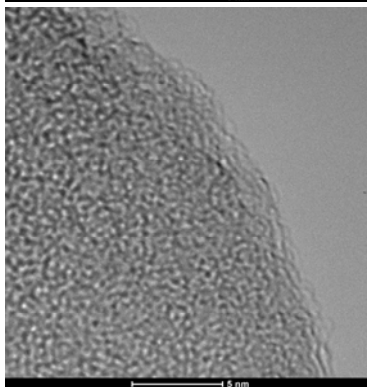
71-39_C60_Ozopolym_450_N2



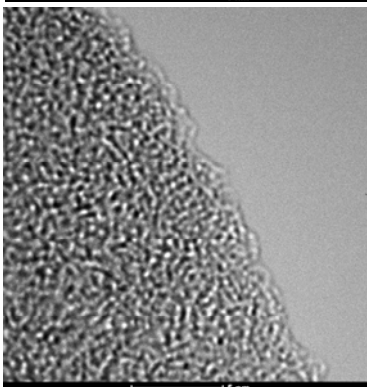
71-39_C70_Ozopolym_450_N2



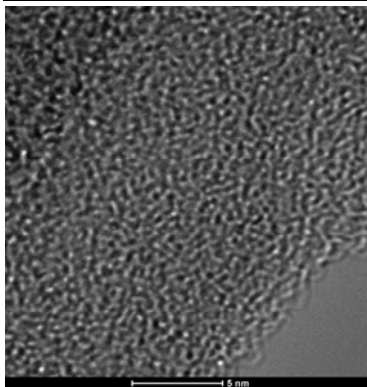
71-39_C60_Ozopolym_630_N2



71-39_C70_Ozopolym_630_N2



77-38_C60_Ozopolym_CHCl3



The structural differences among the probes of **Table 1** may be understood in terms of forming of micro-currents, yet with a mechanism of special chemical bonding involving the

bondons on the monolayer graphenes [9-11], as extracted from the spectral quantum information, see the next section.

Quantum spectral Raman and AFM information from graphenic monolayers

Graphene oxide are characterized by the presence of hydroxy, epoxy and carboxyl groups which is an important property for obtaining better electrical and mechanical characteristics of the material. Despite the fact that reduced graphene oxide has less functional groups than graphene oxide due to the reduction process, the above mentioned functional groups still exist, in conclusion, hydroxy-epoxy functionalized graphene and graphene oxide are the same material.

Ozonized fullerenes or fullerene ozopolymers that were developed lately also contain oxidized functional groups [13]. These compounds contain open cage graphene structures that are connected to each other by oxigenated bridges, called buckybowls or graphene sheets with fullerene-like structures [9].

Fullerenes (C60 and C70) and trichloromethane (CHCl₃) were of analytical grade and purchased from Sigma Aldrich. The Raman spectrum was measured by the MultiView-2000 system (Nanonics Imaging Ltd., Israel) and incorporated Shamrock 500i Spectrograph (ANDOR, United Kingdom) at room temperature. A laser wavelength of 514.5 nm (19,437 cm⁻¹) as the excitation source was used with 20 s exposure time.

Raman spectroscopy is widely used to evaluate the crystal structure, disordering and defects. Other applications include characterization of conjugated and double carbon-carbon bonds that have significant importance in graphene and other carbon compounds identification [14]. The literature indicates that Stokes phonon energy shift generated by laser excitation creates three main peaks in graphene: G located at 1580 cm⁻¹, D at 1350 cm⁻¹ and 2D at 2690 cm⁻¹ [15]. Typical Raman spectrum for the graphene oxide has G band peak at 1590 cm⁻¹ and D peak around 1350 cm⁻¹. Graphene nano walls have G band peak at 1590 cm⁻¹ indicating the formation of a graphitized structure and D band peak at 1350 cm⁻¹ corresponding to the disorder-induced phonon mode [14,16]. In the case of graphene oxide Raman spectra it was also observed that the G band has the tendency to shift to higher frequency during graphite amorphization [17].

For the probes of **Table 1** the actual Raman spectra were accordingly obtained in the **Figure 5**.

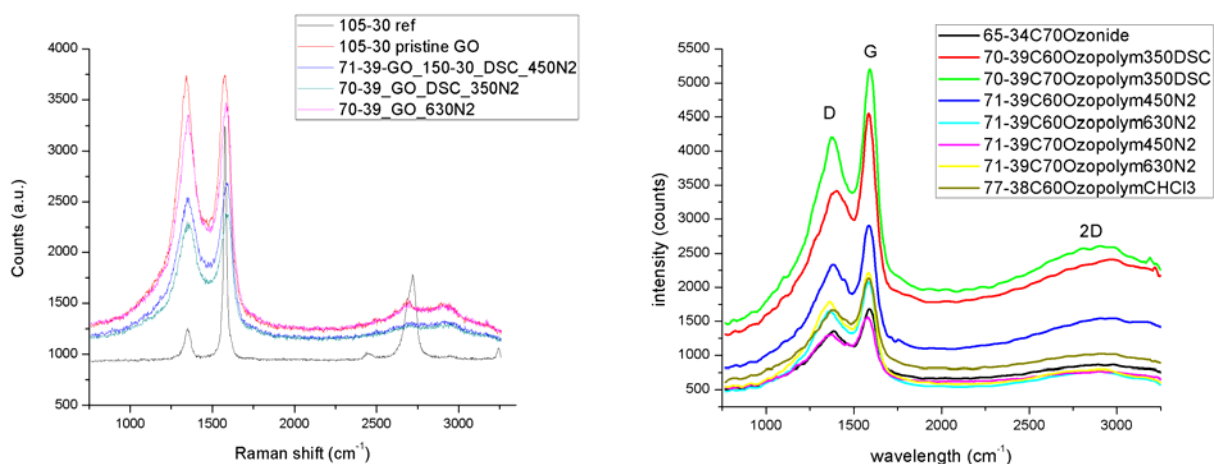


Figure 5. The systematic Raman Stokes bands for the graphenic probes of **Table 1** [18], see the text for details.

The spectral bondonic information was extracted from Figure 5 with the following quantum related algorithm [18]:

- Intensity of formed micro-currents

$$I_B[A] = 1.51146 \times 10^{-7} \frac{\Delta \tilde{\nu}_{FWHM} [cm^{-1}]}{IQ^{3/2}}$$

- The inverse quantum factor [19] is based on the observed vs. free quantum evolution of the quasi-quantum particle of bondon representing the bonds under investigations for the Raman bands of **Figure 5**:

$$IQ_{Obs/Free} = \frac{\left(\frac{Particle}{Wave} \right)_{Observed Evolution}}{\left(\frac{Particle}{Wave} \right)_{Free Evolution}}$$

- The spectral observed particle to wave quantum nature is analytically expressed as:

$$\left(\frac{Particle}{Wave} \right)_{Observed Evolution} = \frac{1}{\sqrt{3+2n^2}} \exp\left(\frac{3+n^2}{6+4n^2}\right)$$

- The free particle to wave quantum nature is analytically expressed as:

$$\left(\frac{Particle}{Wave} \right)_{Free Evolution} = \frac{1}{\sqrt{3-2n^2}} \exp\left(\frac{3-3n^2}{6-4n^2}\right)$$

- With the quantum fluctuation factor (n) through considering, respectively as:

$$n_{Obs} = \frac{1}{\tilde{\nu}_0 \sqrt{\frac{1}{\Delta \tilde{\nu}_{FWHM}^2} + \frac{1}{4} \left(\frac{1}{\tilde{\nu}_L^2} + \frac{1}{\tilde{\nu}_R^2} + \frac{2}{\tilde{\nu}_L \tilde{\nu}_R} \right) - \frac{1}{\tilde{\nu}_0^2}}}$$

and

$$n_{Free} = \frac{1}{\tilde{\nu}_0 \sqrt{\frac{1}{\Delta \tilde{\nu}_{FWHM}^2} + \frac{1}{4} \left(\frac{1}{\tilde{\nu}_L^2} + \frac{1}{\tilde{\nu}_R^2} + \frac{2}{\tilde{\nu}_L \tilde{\nu}_R} \right) + \frac{1}{\tilde{\nu}_0^2}}}$$

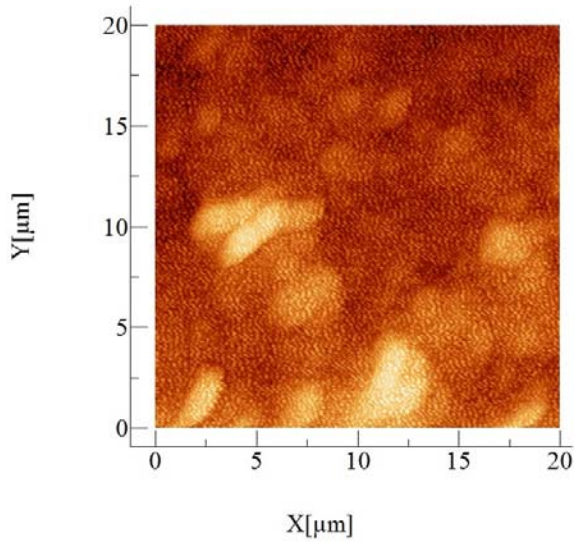
With $\tilde{\nu}_0(A_{max})$ as the maximum intensity's line wave-number, $\tilde{\nu}_L, \tilde{\nu}_R$ the spectral left and right wave-numbers of the working spectral band, and $\Delta \tilde{\nu}_{FWHM}$ the full width of a half maximum (FWHM) wave-number of the concerned spectral band is reciprocally associated with the dispersion of the quantum paths of vibrations within the band.

The micro-currents obtained within the graphenic monolayers by the present quantum bondonic theory for the probes of are in **Table 2** systematically presented.

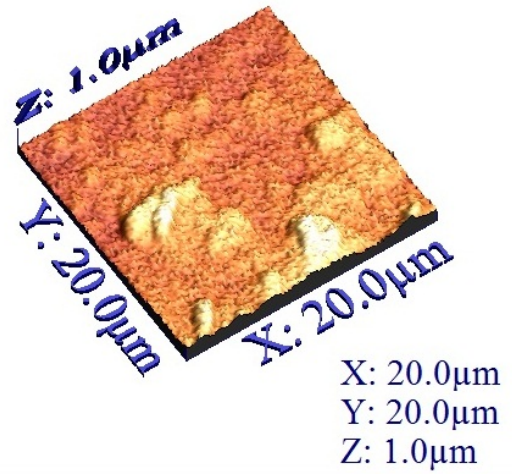
Table 2. The Raman Spectral-IQ results [18], as based on the bondonic spectral IQ formalism for the bands of Figures 5 and 6 for the graphenic probes of **Table 1**.

Probe	Peaks of interest	$\tilde{\nu}_L$	$\tilde{\nu}_R$	$\tilde{\nu}_0(A_{\max})$	$\Delta\tilde{\nu}_{FWHM}$	IQ	$I_B[\mu A]$
105-30_Pristine GO		1185	1482.5	1355	105.00605	0.996026	15.9663
		1482.5	1687.5	1603.7	74.07562	0.998581	11.2201
		2454.1	2957.5	2715.2	268.85261	0.993539	41.033
70-39_GO_630_N2	D	1095.7	1623.8	1341.2	185.19473	0.987576	28.5213
	G	1425.9	1726.1	1572.2	108.71338	0.99683	16.51
	2Da	2488.5	2969.5	2703.4	233.56015	0.995067	35.5645
70-39_GO_DSC_350_N2	D	1177.2	1507.3	1359.7	124.28282	0.994486	18.9413
	G	1519.8	1714.8	1621.6	68.09731	0.998827	10.3108
	2Da	2405	3135	2746	378.50413	0.987611	58.2893
71-39_GO_105-30_DSC_450_N2	D	1024.6	1712.3	1389.4	250.76054	0.979185	39.1164
	G	1452.2	1712.3	1593.3	95.16282	0.997632	14.4347
	2Da	2537.4	2922.7	2719.6	221.70265	0.995604	33.7317
105-30_ref	D	1255.4	1412.4	1354.2	49.7069	0.999103	7.52312
	G	1501.7	1667.2	1579.7	24.89621	0.999834	3.7639
	2Db	2585	2828.5	2723.5	78.73974	0.999443	11.9111
65-34_C70_Ozonide	D	981.23	1801.5	1396.4	364.68625	0.958361	58.752
	G	1453	1744	1589	73.23262	0.998587	11.0923
	2Da	2274	3234.6	2864.4	595.36851	0.97273	93.798
70-39_C60_Ozopolym_350_DSC	D	957.45	1561.4	1433.4	418.7584	0.949915	68.3648
	G	1562	1626.4	1591.4	83.42495	0.998174	12.644
	2Da	2821.9	3089.5	3400	34.6314	0.999931	5.23494
70-39_C70_Ozopolym_350_DSC	D	1143.9	1629.1	14115	237.339	0.999817	35.8827
	G	1504.1	1684.2	1591.6	88.84143	0.99793	13.4698
	2Da	1751.7	3500	2947.5208	1387.23428	0.892649	248.614
71-39_C60_Ozopolym_450_N2	D	1156.3	1606.4	1393.9	188.47564	0.98808	29.0044
	G	1483.9	1714	1586.4	87.24385	0.997991	13.2264
	2Da	2019.1	3247.1	3029.5	1010.95878	0.937038	168.459
71-39_C70_Ozopolym_450_N2	D	1196.3	1531.4	1381.3	188.22045	0.987895	28.9733
	G	1488.9	1689	1593.9	103.13216	0.997223	15.6532
	2Da	2286.7	3262.1	2859.4	722.95703	0.960591	116.065
71-39_C60_Ozopolym_630_N2	D	991.23	1736.5	1393.9	296.03025	0.97168	46.7141
	G	1466.4	1701.5	1588.9	90.18007	0.997861	13.6742
	2Da	2141.7	3252.1	2905.7	852.38343	0.948803	139.401
71-39_C70_Ozopolym_630_N2	D	1203.8	1471.4	1361.3	118.75643	0.994973	18.0858
	G	1476.4	1724	1601.4	87.05715	0.998037	13.1972
	2Da	2119.1	3262.1	2999.5	927.94724	0.944183	152.875
77-38_C60_Ozopolym_CHCl3	D	1233.8	1606.4	1416.4	330.79969	0.965827	52.676
	G	1538.9	1646.5	1586.4	80.94357	0.99827	12.2661
	2Da	2051.6	3232.7	3038.6	1474.00425	0.885308	267.457

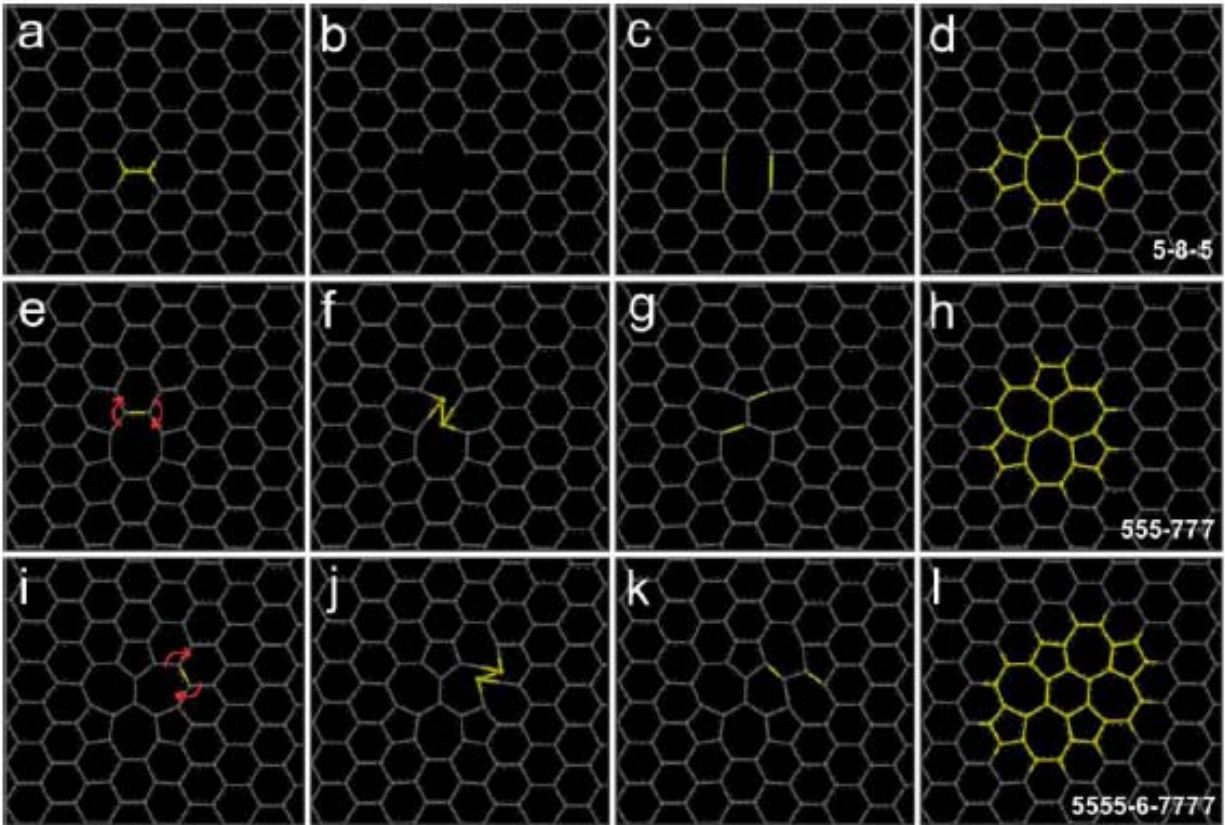
The quantum physical phenomenology of obtained micro-currents (last column) of **Table 2** is the most promising result so far in the project, since highly depended and varying on the graphenic structure under concern It can nevertheless may be based on the first line of scientific research of the present project, namely understanding of the role of topological vs. structural defects and topological isomerisation and inner propagation (viz. micro-currents' formations) within the graphenic lattice.



The AFM of probe 1 in Table 1 [20].



The 3D of probe 1 (of Table 1) in water [20].



The 585 Stone-Wales isomerisation evolution through the graphenic inner bonding transitions [21].

Figure 6. The phenomenological route of explanation for the observed AFM impurities on graphenic probes by the topologically driving the structural defects on the graphenic grids by the Stone-Wales rotation's phase-transition of inner self-isomerizations.

The immediate next proposed line of study will be combining the Stone-Wales rotations within the graphenic supercells and of their propagation with the Atomic Force Microscopy (AFM) systemically measurements, **Figure 6**, on the relevant probes with the maximum quantum current yields.

Yet, the topological vs. structural defects on graphenic monolayer and on the multigraphene layers systems may concede fruitful green technological application as based on non-toxic carbon based materials, see the next sections. Page | 11

Technical Progress: Green applications

Photovoltaic Graphenic Semiconductors

Graphene as a single-atom-thick honeycomb lattice of carbon atoms has extraordinary optical and electrical features like high electron mobility (100 times greater than silicon). This makes it an attractive material for applications in photovoltaic devices. However, such extremely conductive quality negatively impacts on life-time efficiency in photovoltaics' life cycle, when accordingly incorporated. The present challenge is to design and exploit *semiconductor-graphene* (SG), with controlled conductivity that assuring the desired energy conversion also maintains the long life using photovoltaics. Accordingly, two new forms of graphene are studied and employed, as new classes of n-doped, and p-doped semiconductors, so producing the so called, e-SG (electron-type semiconductor graphene, based on *topological defective* Graphene, as appeared by inherent Stone-Wales topological rotations in pristine Graphene 0-G) and h-SG (hole-type semiconductor graphene, when the *structurally defective* graphene is present), see **Figure 7** [22].

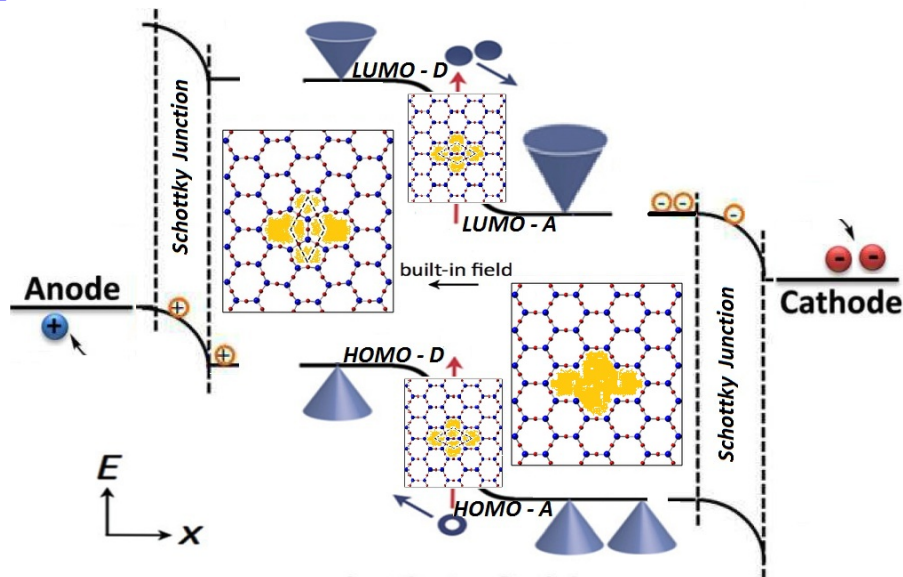


Figure 7. Schematic representation of the photovoltaic photocurrent generation mechanism by donor-interlayer-acceptor heterojunction on the graphene base using the isomorphous forms of topologically defective graphene vs. structurally defective graphene states recombined in the inter-layer region by the pristine graphene, respectively [22].

This way, the new controlled photovoltaic systems may be composed from various layers of pristine and semiconductor graphenes, passing from the fashioned generation of i-/p-/n-semiconductor based heterojunctions photovoltaics to the new generation of e-/h-SG controlled photovoltaics based on defective semiconductor graphenes – for a long-life use. The efficiency of photovoltaic materials with 0-G, e-SG, and h-SG heterojunctions is to be next explored by using computational quantum chemistry methods.

Molecular Machines activated by Light

Other intriguing PV-related study, may starting on the one side from the main features of molecular machines and on the other side from the applicability of Fredholm integral in electrochemistry, in order to set up quantum electrochemical models with applicability in molecular machines field [23], and represents the first part of a series of studies regarding this subject. To this aim, one notes the chemical reactivity could be expressed as a link between electronegativity (χ), number of exchanged/carried/transported electrons/charges (N) and the total energy of the system, dynamically evolving under potential V , respectively through the differential equation $\chi = -(\partial E / \partial N)_V$ and/or by its integral form $E = -\int \chi(N)_V dN$. This way, the complementary electrochemistry processes, i.e. electrode interfaces' processes (such as deposition, corrosion, oxidation, reduction processes, etc.) and the electrolyte solution phenomena (diffusion, dispersion, recombination processes, etc.), may be either interchanged and/or separately controlled, respectively (see the **Figure 8** [24]).

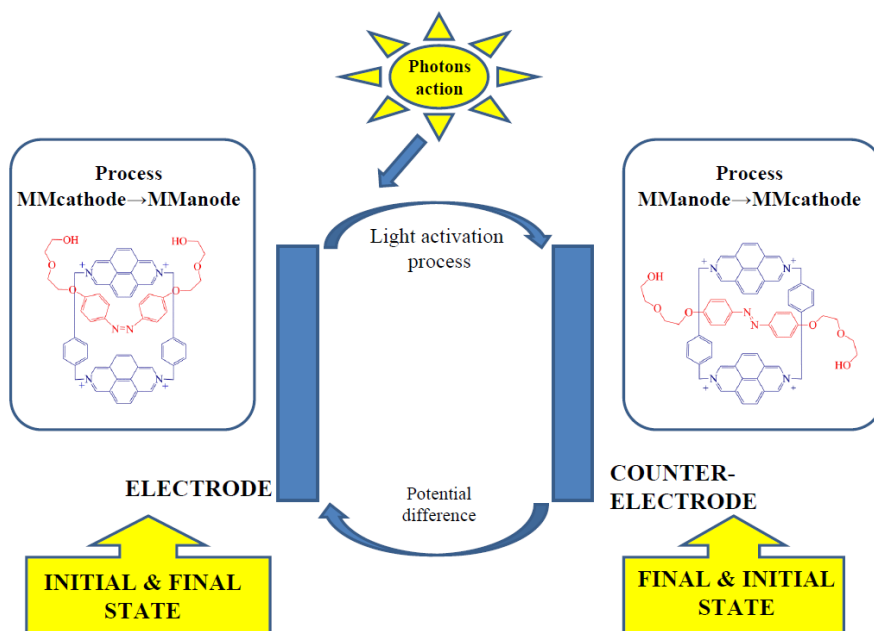


Figure 8. Integration of modules 1 (i.e. the correspondence of the differential with the integral formulation of the chemical reactivity driven by the electronegativity) & 2 (i.e. application of electrochemical – chemical reactivity integral code to cyclic molecular processes modelling) in an electro-photo-chemical sample [24].

While employing this correspondence scheme, by rewriting the fundamental laws of electrochemistry in terms of electronegativity, the so called *modular electrochemical reactivity laws* are established. Remarkably, such modular controlling of electrochemical processes applied to self-organized molecular machines may control and eventually enhance the life-cycle of photovoltaics, by designing the appropriate *electro-molecular modular photovoltaics machine* with the inner electrochemistry modularly controlled. However, the connection with the photo-active molecular machines triggered by the graphenic inter-double-layers as electrodes and counter electrodes (viz. topological vs. structural defective graphenes) is the next challenge to be faced in the 2018 research phase of the present experimental project.

Conclusions and 2018 Perspectives

Topological assessment of molecules is particularly important for big structures where the component atoms present sophisticated connectedness. Topological studies are, in fact, the first studies which are trying to explain or to predict the physical-chemical properties of the molecule and/or its eventual biological activity. Carbon allotropes like graphene sheets, fullerenes and fullerene derivatives are molecules presenting a high number of atoms connected between them in a complicated network, with connection patterns, like in a crystalline material and also possible structural defects. In this context, there appears clearly now that in the case of these structures we can speak about a spatial dimensionality which refers to spatial geometry of molecules but also about a Wiener dimensionality which refers to the “connection degree” of an atom and its involvement into “open-ends” or “closed-ends” atomic networks: a graph with “closed ends” presents more (or all) atoms with the same topological symmetry and this means that the structure has an increased compactness and a higher energetic stability. In terms of chemical reactivity, the higher the molecular compactness is, the more inert the molecule is. This principle can also be applied for “internal” and “marginal” atoms in a molecule. The marginal atoms in the molecule can be easier substituted or derivatized than the “hidden” ones. In fullerenes and nanotubes, the structures cannot present only hexagonal “honeycomb” cells but also pentagonal ones, for the structure to enclose and spatially resemble a “cage” or a “cylinder”; therefore, for the graphene oxides and graphenes derived from fullerenes controlled crackings [9-11] in this respect, the authors of Ref. [3] describe intrastructure isomerisation possibilities which can propagate in a certain direction, with exchanging bond (edge) positions and reforming the cell patterns not only locally but in the whole molecule. They are widely confirmed by experimentally recording of a series of associated HRTEM films [12]. So, the topo-structural studies will be continuing being a mathematically structural tool for assessing and interpreting the observed morphology of carbon-based materials in general and of graphenic sheets and multilayers in special.

Advances in green nano-technologies is the main field under which the present paper series is firstly envisaged; therefore, advanced, research-progressive nano-science is aimed to shorten the distance from fundamental concepts to applications, devices and their implementations. It however gather both physics and chemistry fundamental and applicative fields in dealing with solar/black body radiation as well as with new materials based on inorganic-organic hybrids, composites and electron quantum features (excitons, bondons, diffusion, electrical circuits, semiconductors, quantum dots, etc.). Such research is therefore equally highly necessary for both communities (physical engineering and chemical engineering)

enlightening the dedicated international forums on quantum-dots based solar cells, as well as for giving further impetus to this new field of photovoltaics by gathering active international scientist in solar energy [25].

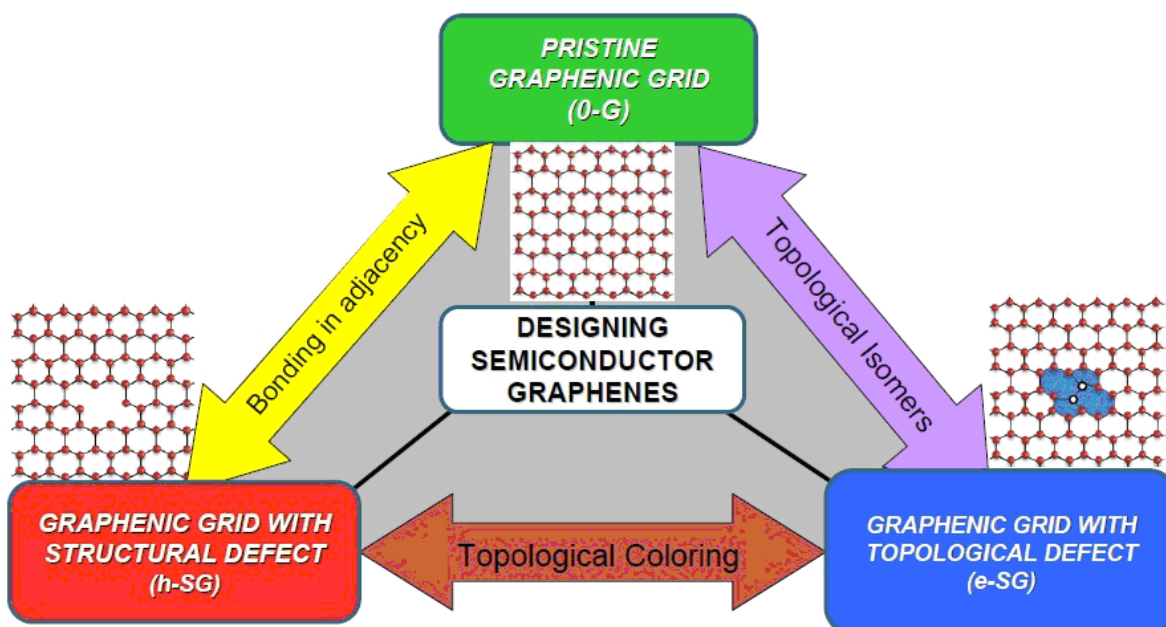


Figure 9. Conceptual and structural inter-relation of three forms of graphene used in binding the semiconductor graphenic systems, emphasising on the physical-chemistry operations bringing one form to another [22,25].

This general framework fortunately may combine with the recently advanced *bondonic* quasi-quantum particle [26] modelling the chemical bonding field on graphenic monolayers (see the Raman spectra analysis and the further AFM vs. 585 Stone-Wales evolutions above), to be by this project on 2018 further generalized to the *bondots* – the particles of *coherently* bonding of quantum dots appeared in condensed matter, multigraphene inclusive as starting from the bi-layer case studies first on 2018, eventually reshaping the electronics by advancing the graphenic semiconductors, see above section and also the **Figure 9**, in the first instance and the *graphentronics* at large afterwards. Since the quantum-dots (QD) have been already proved with their sensitizing potential on solar cells the present *double*-quantum dots (bondotic) –DQD approach may yield further (at least *doubling*) the solar photovoltaic performances of the energy materials working with such mechanism.

References

1. Iijima, S. (1980) Direct observation of the tetrahedral bonding in graphitized carbon black by high resolution electron microscopy, *Journal of Crystal Growth*, 50(3), 675-683.
2. Cataldo, F.; Ori, O.; Graovac, A. (2013) Graphene topological modifications. In: *Advances in Chemical Modeling (Chemistry Research and Applications)* Putz, M.V. Ed., Nova, New York, 3, 241–260.
3. Bumbăcilă B., Ori O., Cataldo F., Putz M.V. (2017) Topological Modeling of Carbon Nano-Lattices, *Current Organic Chemistry* 21 000-000;

- DOI: 10.2174/1385272821666170428123839; (ISI Impact Factor ~ 2);
 URL: <http://www.eurekaselect.com/152007>.
4. Ori, O.; Cataldo, F.; Vukičević, D.; Graovac, A. (2010) Wiener Way to Dimensionality, *Iranian Journal of Mathematical Chemistry*, 1(2), 5-15.
 5. Mohar, B.; Pisanski, T. (1988) How to compute the Wiener index of a graph, *Journal of Mathematical Chemistry*, 2(3), 267-277.
 6. Ori, O.; Putz, M.V.; Gutman, I.; Schwerdtfeger, P. (2014) Generalized Stone-Walls Transformations for Fullerene Graphs Derived from Berge's Switching Theorem. In: *Ante Graovac – Life and Works* Gutman, I.; Pokrić, B.; Vikičević, D. (Eds.), *Mathematical Chemistry Monographs*, 16, University of Kragujevac, Chapter 5, Part C, 259-272.
 7. Babić, D.; Bassoli, S.; Casartelli, M.; Cataldo, F.; Graovac, A.; Ori, O.; York, B. (1995) Generalized Stone-Walls transformations, *Molecular simulation*, 14, 395-401.
 8. Ori, O.; Cataldo, F.; Putz, M.V. (2011) Topological Anisotropy of Stone-Wales Waves in Graphenic Fragments, *International Journal of Molecular Sciences*, 12, 7934-7949.
 9. Cataldo F., Putz M.V., Ursini O., Angelini G., Garcia-Hernandez A., Manchado A. (2016) A New Route to Graphene Starting from Heavily Ozonized Fullerenes: Part 1 – Thermal Reduction under Inert Atmosphere. *Fullerenes, Nanotubes and Carbon Nanostructures*. 24 (1), 52-61; DOI: 10.1080/1536383X.2015.1101535.
 10. Cataldo F., Putz M.V., Ursini O., Angelini G., Garcia-Hernandez A., Manchado A. (2016) A New Route to Graphene Starting from Heavily Ozonized Fullerenes: Part 2 – Oxidation in Air. *Fullerenes, Nanotubes and Carbon Nanostructures*. 24 (1), 62-66; DOI: 10.1080/1536383X.2015.1110697.
 11. Cataldo F., Putz M.V., Ursini O., Angelini G., Garcia-Hernandez A., Manchado A. (2016) A New Route to Graphene Starting from Heavily Ozonized Fullerenes: Part 3 – An Electron SPIN Resonance Study. *Fullerenes, Nanotubes and Carbon Nanostructures*. 24(3), 195-201; DOI: 10.1080/1536383X.2015.1113524.
 12. Putz M.V., Taranu B., Balcu I., Cataldo F. Quantum particles on graphenic systems. Part 3. *Bondons by TEM morphology, Fullerenes, Nanotubes, and Carbon Nanostructures (FNCN)*. in preparation, to be submitted.
 13. Cataldo, F. (2003) Structural Analogies and Differences Between Graphite Oxide and C60 and C70 Polymeric Oxides (Fullerene Ozopolymers), *Fullerenes, Nanotubes, Carbon Nanostruct.*, 11(1), 1-13.
 14. Kudin, K.N., Ozbas, B., Schniepp, H.C., Prud'homme, R.K., Aksay, I.A., Car, R. (2008) Raman Spectra of Graphite Oxide and Functionalized Graphene Sheets. *Nano Letters*, 8(1), 36-40.
 15. Childres, I., Jauregui, L.A., Park, W., Cao, H. and Chen, Y.P. (2013) Raman Spectroscopy of Graphene and Related Materials. In *Developments in Photon and Materials Research*, Jang J.I. (Ed.), Nova Science Publishers, New York, 19, 1-20.
 16. Hiramatsu, M., Kondo, H. and Hori, M. (2013) Graphene Nanowalls. *Nanotechnology and Nanomaterials*. In: *New Progress on Graphene Research*, Gong J.R. (Ed.), 9, 235-260, DOI: 10.5772/51528.
 17. Kim, K.S., Zhao, Y., Janget, H. (2009) Large-scale pattern growth of graphene films for stretchable transparent electrodes. *Nature*, 457, 706-710.
 18. Putz M.V., Svera P., Putz A.M., Cataldo F. Quantum particles on graphenic systems. Part 2. Bondons by absorption Raman spectra, *Fullerenes, Nanotubes, and Carbon Nanostructures (FNCN)* submitted, to be accepted (ISI Impact Factor ~ 1.35).

19. Putz A.M., Putz M.V. (2012) Spectral Inverse Quantum (Spectral-IQ) Method for Modeling Mesoporous Systems. Application on Silica Films by FTIR. *International Journal of Molecular Sciences*, 13(12) 15925-15941; DOI:10.3390/ijms131215925.
20. Putz M.V., Iorga M.I., Svera P., Novaconi S., Cataldo F. Quantum particles on graphenic systems. Part 4. *Bondots by photovoltaic metrology. Fullerenes, Nanotubes, and Carbon Nanostructures (FNCN), in preparation, to be submitted.*
21. Putz M.V., Ori, F., Et Al. Quantum particles on graphenic systems. Part 5. Semiconductor Graphenes by Topological Defects. *Fullerenes, Nanotubes, and Carbon Nanostructures (FNCN), in preparation, to be submitted.*
22. Buzatu D.L., Mirica M.C., Putz M.V. (2017) Semiconductor Graphenes for Photovoltaics. In: *Nearly Zero Energy Communities, Proceedings of the Conference for Sustainable Energy (CSE) 2017*, Visa I., Duta A. (Eds.), Springer Proceedings in Energy, 348-363, DOI 10.1007/978-3-319-63215-5_25; Hardcover ISBN:978-3-319-63214-8; eBook ISBN:978-3-319-63215-5. Springer International Publishing AG 2018 (Cham, Switzerland); URL: <http://www.springer.com/gp/book/9783319632148>
23. Venturi M., Iorga M.I., Putz M.V. (2017) Molecular devices and machines: hybrid organic-inorganic structures, *Current Organic Chemistry*, 21 000-000; DOI: 10.2174/1385272821666170531121733; (ISI Impact Factor ~ 2); URL: <http://www.eurekaselect.com/152818>.
24. Iorga M.I., Mirica M.C., Putz M.V. (2017) Modular Electrochemical Reactivity for Photovoltaics' Machines. In: *Nearly Zero Energy Communities, Proceedings of the Conference for Sustainable Energy (CSE) 2017*. Visa I., Duta A. (Eds.), Springer Proceedings in Energy, 405-420, DOI 10.1007/978-3-319-63215-5_25. Hardcover ISBN:978-3-319-63214-8; eBook ISBN:978-3-319-63215-5. Springer International Publishing AG 2018 (Cham, Switzerland); URL: <http://www.springer.com/gp/book/9783319632148>
25. Putz M.V., Buzatu D.L., Mirica M.C., Ori O. Quantum particles on graphenic systems. Part 1. Roadmap to semiconductor based graphenes, *Fullerenes, Nanotubes, and Carbon Nanostructures (FNCN), submitted, to be accepted* (ISI Impact Factor ~ 1.35);
26. Putz M.V., Cimpoesu F., Ferbințeanu M. *Structural Chemistry: Principles, Methods, And Case Studies On The Molecular And Nanoscale* (2017/2018) Springer Verlag, Dordrecht, NL, E-Book ISBN: 978-3-319-55875-2; Hard-Book ISBN: 978-3-319-55873-8; pp. ~ 800+index; URL: <http://www.springer.com/gp/book/9783319558738>